# BRAIN
## A JOURNAL OF NEUROLOGY

# Tissue-resident memory T cells invade the brain parenchyma in multiple sclerosis white matter lesions

Nina L. Fransen,[1] Cheng-Chih Hsiao,[2] Marlijn van der Poel,[1] Hendrik J. Engelenburg,[1] Kim Verdaasdonk,[1] Maria C.J. Vincenten,[1] Ester B.M. Remmerswaal,[2,3] Tanja Kuhlmann,[4] Matthew R.J. Mason,[1] Jörg Hamann,[1,2,*] Joost Smolders[1,5,*] and Inge Huitinga[1,6,*]

*These authors contributed equally to this work.

Multiple sclerosis is a chronic inflammatory, demyelinating disease, although it has been suggested that in the progressive late phase, inflammatory lesion activity declines. We recently showed in the Netherlands Brain Bank multiple sclerosis-autopsy cohort considerable ongoing inflammatory lesion activity also at the end stage of the disease, based on microglia/macrophage activity. We have now studied the role of T cells in this ongoing inflammatory lesion activity in chronic multiple sclerosis autopsy cases. We quantified T cells and perivascular T-cell cuffing at a standardized location in the medulla oblongata in 146 multiple sclerosis, 20 neurodegenerative control and 20 non-neurological control brain donors. In addition, we quantified $CD3^+$, $CD4^+$, and $CD8^+$ T cells in 140 subcortical white matter lesions. The location of $CD8^+$ T cells in either the perivascular space or the brain parenchyma was determined using CD8/laminin staining and confocal imaging. Finally, we analysed $CD8^+$ T cells, isolated from fresh autopsy tissues from subcortical multiple sclerosis white matter lesions ($n = 8$), multiple sclerosis normal-appearing white matter ($n = 7$), and control white matter ($n = 10$), by flow cytometry. In normal-appearing white matter, the number of T cells was increased compared to control white matter. In active and mixed active/inactive lesions, the number of T cells was further augmented compared to normal-appearing white matter. Active and mixed active/inactive lesions were enriched for both $CD4^+$ and $CD8^+$ T cells, the latter being more abundant in all lesion types. Perivascular clustering of T cells in the medulla oblongata was only found in cases with a progressive disease course and correlated with a higher percentage of mixed active/inactive lesions and a higher lesion load compared to cases without perivascular clusters in the medulla oblongata. In all white matter samples, $CD8^+$ T cells were located mostly in the perivascular space, whereas in mixed active/inactive lesions, 16.3% of the $CD8^+$ T cells were encountered in the brain parenchyma. $CD8^+$ T cells from mixed active/inactive lesions showed a tissue-resident memory phenotype with expression of CD69, CD103, CD44, CD49a, and PD-1 and absence of S1P1. They upregulated markers for homing (CXCR6), reactivation (Ki-67), and cytotoxicity (GPR56), yet lacked the cytolytic enzyme granzyme B. These data show that in chronic progressive multiple sclerosis cases, inflammatory lesion activity and demyelinated lesion load is associated with an increased number of T cells clustering in the perivascular space. Inflammatory active multiple sclerosis lesions are populated by $CD8^+$ tissue-resident memory T cells, which show signs of reactivation and infiltration of the brain parenchyma.

1 Department of Neuroimmunology, Netherlands Institute for Neuroscience, Amsterdam, The Netherlands
2 Department of Experimental Immunology, Amsterdam Infection and Immunity Institute, Amsterdam University Medical Centers, Amsterdam, The Netherlands
3 Renal Transplant Unit, Department of Internal Medicine, Amsterdam University Medical Centers, Amsterdam, The Netherlands
4 Institute for Neuropathology, University Hospital Münster, Münster, Germany
5 MS center ErasMS, Departments of Neurology and Immunology, Erasmus Medical Center, Rotterdam, The Netherlands
6 Swammerdam Institute for Life Sciences, University of Amsterdam, Amsterdam, The Netherlands

Correspondence to: Joost Smolders
MS center ErasMS, Departments of Neurology and Immunology
Erasmus Medical Centre, Rotterdam, The Netherlands
E-mail: j.j.f.m.smolders@erasmusmc.nl

Correspondence may also be addressed to: Inge Huitinga
E-mail: i.huitinga@nin.knaw.nl

# Introduction

Relapsing-remitting multiple sclerosis is at its onset characterized by a relatively high frequency of clinical exacerbations and gadolinium-enhancing lesions on brain MRI (McFarland *et al.*, 1996; Vollmer, 2007; Thompson *et al.*, 2018). These phenomena are believed to reflect waves of inflammatory cells trafficking from the circulation through the blood–brain barrier into the CNS causing focal demyelinating lesions. Invading T cells have been proposed to play a central role in the early disease process of multiple sclerosis (Dendrou *et al.*, 2015). At later stages, both relapse rate and lesion enhancement often decline to near zero (McFarland *et al.*, 1996; Vollmer, 2007; Thompson *et al.*, 2018). Patients with advanced multiple sclerosis often experience a continuous deterioration of neurological functions referred to as progressive multiple sclerosis (Thompson *et al.*, 2018). Clinical trials of drugs targeting circulating leucocytes are mostly negative on their primary end points in progressive multiple sclerosis. Advanced multiple sclerosis is therefore sometimes referred to as a disease driven by neurodegenerative mechanisms rather than inflammatory mechanisms (Mahad *et al.*, 2015).

When performing an immunohistochemical analysis of a large collection of post-mortem multiple sclerosis brains, we encountered mixed active/inactive (previously referred to as chronic active) lesions containing HLA$^+$ macrophages in 78% of brain donors with advanced multiple sclerosis (Luchetti *et al.*, 2018). In this autopsy cohort, the percentage of mixed active/inactive lesions correlated with a faster accrual of multiple sclerosis-related disability (Luchetti *et al.*, 2018). Earlier studies suggest a role of T cells in this ongoing inflammatory response in patients with chronic multiple sclerosis, as perivascular inflammatory infiltrates are found in association with mixed active/inactive lesions, specifically in secondary progressive multiple sclerosis cases (Revesz *et al.*, 1994). These T cells mostly express CD8 (Booss *et al.*, 1983; Hayashi *et al.*, 1988; Frischer *et al.*, 2009; van Nierop *et al.*, 2017; Machado-Santos *et al.*, 2018) and display signs of clonal expansion (Babbe *et al.*, 2000). Whether T cells also critically contribute to the ongoing inflammation in advanced multiple sclerosis, where signs of trafficking immune cells through the blood–brain barrier are generally lacking, is uncertain.

Recently, we characterized T cells in normal human brain white matter by flow-cytometric analysis of rapid post-mortem autopsy tissue (Smolders *et al.*, 2013, 2018). We observed low numbers of predominantly CD8$^+$ T cells, almost exclusively residing in the perivascular space (PVS), with a phenotype resembling the core profile of tissue-resident memory T ($T_{RM}$) cells (Smolders *et al.*, 2018). In several tissues, viral antigen-specific CD8$^+$ $T_{RM}$ cell populations that arise after a first viral infection are characterized by a set of surface markers including the C-type lectin CD69 and the alpha E integrin CD103. These cells do not recirculate but are retained locally to become reactivated in the case of renewed viral exposure (Szabo *et al.*, 2019). CNS $T_{RM}$ cell populations also develop after experimental neurotropic virus infection (Aguilar-Valenzuela *et al.*, 2018; Schøller *et al.*, 2019; Shwetank *et al.*, 2019). Evidence suggests that multiple sclerosis-associated T-cell populations express markers associated with $T_{RM}$ cells. Sørensen *et al.* (1999) found both CXC chemokine receptor (CXCR)3 and C-C chemokine receptor (CCR)5 expression by perivascular cuff and lesional T cells. Machado-Santos *et al.* (2018) described a loss of the recirculation markers sphingosine-1-phosphate receptor 1 (S1P1) and CCR7, and an upregulation of CD103 and CCR5, but not CD69, by lesional CD8$^+$ T cells. Contrastingly, van Nierop *et al.* (2017) found no expression of CD103 but rather expression of CD69 by CD8$^+$ T cells. Whether white matter lesion-associated T cells are *bona fide* $T_{RM}$ cells and contribute as such to chronic multiple sclerosis lesion activity remained to be consolidated.

We here used a combination of immunohistochemistry and flow cytometry to study the localization, quantity, and phenotype of CD8$^+$ T cells in association with multiple sclerosis normal-appearing white matter and white matter lesions.

# Material and methods

## Donors and tissue characteristics

One hundred and forty-six multiple sclerosis brain donors from the Netherlands Brain Bank were included in the analysis of T cells in multiple sclerosis lesions. Informed consent was given by the donors for brain autopsy and for the use of material and clinical data for research purposes, in compliance with national ethical guidelines. The Netherlands Brain Bank autopsy procedures were approved by the

Medical Ethics Committee of the VU Medical Center, Amsterdam, The Netherlands. The donors came to autopsy between 1991 and 2015. The clinical diagnosis of multiple sclerosis was confirmed for all patients, and the clinical course was defined as relapsing (for both relapsing-remitting and progressive relapsing cases), secondary progressive, or primary progressive by a certified neurologist according to McDonald or Poser criteria. The diagnosis of multiple sclerosis was confirmed by a certified neuropathologist.

T cells and perivascular cuffing were examined in the standardly dissected brainstem at the level of the medulla oblongata. The brainstem allowed a standardized comparison between multiple sclerosis autopsy cases in a functionally important white matter tract. Brainstem tissue blocks were obtained from 146 multiple sclerosis cases, 20 Alzheimer's disease cases (Braak score >5), and 20 non-neurological controls (Table 1). To correlate T-cell numbers with stages of multiple sclerosis lesion pathology, subcortical white matter lesions were studied. Subcortical white matter tissue blocks from 57 multiple sclerosis donors containing 140 multiple sclerosis white matter lesions were obtained together with subcortical white matter from 20 Alzheimer's disease cases (Braak score >5) and 18 non-neurological controls. Treatment status for immunomodulatory therapies (fingolimod, natalizumab, or interferon beta) in the year before death was obtained from the clinical files. From the total 146 multiple sclerosis cases, one had received fingolimod.

Biopsy tissue sections containing inflammatory active multiple sclerosis lesions from six donors were made available by the Institute for Neuropathology, University Hospital Münster, Germany upon approval by the local Medical Ethics Committee. For donor information, see Supplementary Table 1.

## Characterization of multiple sclerosis lesion activity and perivascular T cell cuffing

All brainstem and subcortical white matter tissue sections were immunostained for proteolipid protein (PLP) and human leucocyte antigen (HLA-DR/DQ, referred to as HLA) as previously described (Luchetti *et al.*, 2018; Fransen *et al.*, 2019). Reactive, active, mixed active/inactive, inactive and inactive remyelinated lesions were distinguished. Lesions were annotated, and adjacent sections were stained for CD3 and counterstained with cresyl violet. All tissue sections were systematically examined with the microscope at $\times 20$ magnification, while the observer was blind for the clinical disease course. Perivascular T cell cuffing was considered present when more than one ring of CD3$^+$ T cells was present in the PVS (Revesz *et al.*, 1994).

## Immunohistochemistry and quantification of T cell numbers

Adjacent 8-µm formalin-fixed, paraffin-embedded sections were immunostained for CD3, CD4, and CD8 without nuclear counterstaining. Antigen retrieval was accomplished with microwave treatment at 700 W. Endogenous peroxidase activity and non-specific binding were blocked as described previously (Fransen *et al.*, 2019). Sections were incubated with a primary antibody overnight in blocking buffer at 4°C (details on primary antibodies and concentrations are provided in Supplementary Table 2). The appropriate biotinylated, secondary antibody was applied, followed by conjugation with avidin-biotin horseradish peroxidase (HRP) complex (Vector Elite ABC kit; Vector Laboratories). Alternatively, an anti-rabbit secondary antibody directly conjugated with HRP (REAL™ EnVision™ Detection System; Dako) was applied to the CD8-stained sections. Visualization was established with 3,3′-diaminobenzidine chromogen.

Brightfield tiled images of tissue sections were taken using an Axioscope microscope (Zeiss) while using a green filter to obtain monochromatic light with a $10\times$ Zeiss Plan-Neofluar objective and a black and white camera (XC-77; Sony). To outline the lesions and the normal-appearing white matter, an overlay was made in Adobe Photoshop CC (version 19.1.2; Adobe Systems, San Jose, CA, USA) of the CD3-, CD4-, and CD8-stained sections with the corresponding images of the HLA-PLP-stained section. Areas of interest were manually outlined with Image-Pro Plus 6.3 software (Media Cybernetics, Rockville, MD, USA). For each staining, the background optical density (OD) was measured for all sections. Subsequently, the OD threshold for a positive cell signal was set at four times the average background. OD

**Table 1 Donor and sample information for immunohistochemistry**

| Diagnosis | Cases, n | Age, years | Sex, female/male | PMD, h:min | pH value | Brain weight, g | Disease duration, years |
|---|---|---|---|---|---|---|---|
| Multiple sclerosis | 146 | 64.6 ± 13.1 | 94/52 | 8:58 ± 6:12 | 6.5 ± 0.3 | 1.202 ± 146 | 30.0 ± 13.4 |
| Relapsing-remitting | 15 | 64.2 ± 16.3 | 10/5 | 11:12 ± 13:18 | 6.5 ± 0.4 | 1.214 ± 100 | 24.9 ± 11.8 |
| Primary progressive | 49 | 67.9 ± 13.0 | 31/18 | 8:06 ± 2:27 | 6.5 ± 0.3 | 1.194 ± 132 | 28.6 ± 12.3 |
| Secondary progressive | 82 | 62.8 ± 12.2 | 53/29 | 9:04 ± 5:45 | 6.5 ± 0.3 | 1.186 ± 141 | 31.8 ± 14.2 |
| Neurodegenerative controls (Alzheimer's disease) | 20 | 65.2 ± 6,35 | 11/9 | 5:37 ± 1:41 | 6.5 ± 0.2 | 1.125 ± 183 | – |
| Non-neurological controls | 20 | 63.6 ± 11.0 | 14/6 | 9:08 ± 4:19 | 6.5 ± 0.4 | 1.270 ± 175 | – |

Values are provided as mean ± SD (standard deviation). PMD = post-mortem delay.

particles with size between 10 and 100 µm$^2$ (Downey *et al.*, 1990), exceeding the OD threshold, were counted as CD3$^+$, CD4$^+$, or CD8$^+$ T cells using Image Pro-Plus (Zhu *et al.*, 2016). An example of the mask, created for the particle analysis of CD3 and CD4 immunostainings, is shown in Supplementary Fig. 1. All masks were visually inspected for disturbances.

## Axonal quantification by Bielschowsky silver staining

Axonal density in pyramidal tract normal-appearing white matter was examined in 76 multiple sclerosis and 13 control cases. Bielschowsky silver staining was performed by placing 8-µm thick paraffin-embedded, formalin-fixed tissue sections in Milli-Q$^®$ water, followed by preheated 20% silver nitrate solution, in a dark oven at 40°C. Then, 32% ammonium hydroxide was added until the solution turned colourless, and sections were incubated at 40°C. Next, the sections were placed in 1% ammonium hydroxide solution, and developer solution was added to this solution. The sections were placed in the developer–silver nitrate–ammonium hydroxide solution, followed by fixation in 5% sodium thiosulphate. A grid count was performed at ×40 magnification to quantify axonal density using the Axioscope microscope with a micropublisher 5.0 RTV digital CCD camera (Qimaging) and Image-Pro Plus 6.3 software.

## S1P1 immunohistochemical quantification

Biopsy and autopsy white matter sections were immunostained for S1P1 as described above and in Supplementary Table 2. Tiled images were taken. Using Fiji just ImageJ (Schindelin *et al.*, 2012), the white matter tissue surface area was calculated and the number of positive cells was manually counted.

## Immunofluorescence and confocal imaging

Immunofluorescent double-labelling was performed to analyse multiple sclerosis lesions and perivascular T-cell clusters. Antigen retrieval and incubation with primary antibodies was performed as described above. Sections were then incubated with secondary antibodies directly labelled with Alexa fluorophore Cy3 or Cy5. Alternatively, sections are incubated with biotinylated, secondary antibodies, followed by incubation with streptavidin labelled with Cy3 or Cy5. Anti-CD44 rabbit polyclonal antibody staining was enhanced by Tyramide Signal Amplification (PerkinElmer). Finally, all sections were incubated with Hoechst (33342; Thermo Fisher Scientific). Confocal imaging was performed using the Leica microscope TSA SP8 X at ×20, ×40, and ×63 magnification (Leica Microsystems) using Leica Applications Suite X software (Fransen *et al.*, 2019). For CD8- and

laminin-stained sections, tiled confocal images of tissue sections were made at ×20 magnification (an example is shown in Supplementary Fig. 2).

## Assessment of T cell location

Localization of T cells was assessed in normal-appearing white matter, active, mixed active/inactive, and inactive lesions as described above. Using ImageJ, tissue sections were systematically examined, and the number of parenchymal and perivascular T cells was counted as described in Smolders *et al.* (2018). For donor and tissue information, see Supplementary Table 3.

## Isolation of T cells from fresh autopsy material

White matter from multiple sclerosis and control cases and macroscopically visible multiple sclerosis lesions were dissected at autopsy and stored at 4°C in Hibernate A medium (Invitrogen). A small tissue sample was snap-frozen in liquid nitrogen and stored at –80°C for immunohistochemistry. The remaining tissue was mechanically dissociated as previously described (Smolders *et al.*, 2013, 2018). Mononuclear cells were separated from the suspension by Percoll (GE Healthcare) gradient centrifugation, followed by CD11b magnetic activated cell sorting (Miltenyi Biotech), as previously described (Smolders *et al.*, 2013, 2018; Mizee *et al.*, 2017; van der Poel *et al.*, 2019). After CD11b cell sorting, the flow-through containing T cells was cryopreserved. The frozen tissue sample was sectioned at 20 µm, immunostained for HLA and PLP, and lesions were characterized as described above and in Supplementary Table 2. Donor and sample characteristics are described in Supplementary Table 4. None of the multiple sclerosis cases received immunomodulatory therapies in the year before autopsy.

## Flow cytometric analysis

Cells were stained with antibodies for surface markers and LIVE/DEAD fixable red (Life Technologies) for 30 min at 4°C. Subsequently, cells were washed, fixed, and permeabilized, followed by intracellular staining (Foxp3/ Transcription Factor Staining Buffer Set, Thermo Fisher Scientific). Washed cells were analysed at an LSRFortessa cell analyzer (BD Biosciences). FlowJo software (version 10; Tree Star, Ashland, OR, USA) was used for subsequent data analysis. The guidelines for the use of flow cytometry and cell sorting in immunological studies were followed (Cossarizza *et al.*, 2017). Specifications of the used antibodies are provided in Supplementary Table 5. Gating strategies are shown in Supplementary Fig. 3A. T-distributed stochastic neighbour embedding (t-SNE) analysis was performed with Cytosplore$^{+HSNE}$ software (van Unen *et al.*, 2017).

## Cell sorting and quantitative RT-PCR

Cryopreserved samples were thawed, washed, blocked with 10% normal horse serum, and stained directly with cocktails of fluorescently-conjugated antibodies described in Supplementary Table 5. CD20$^+$ B cells, naïve, memory, effector CD8$^+$ T and natural killer (NK) cells from blood and CD103$^-$ and CD103$^+$CD69$^+$CD8$^+$ T$_{RM}$ cells from brain were sorted on a BD FACS Aria II cell sorter (BD Biosciences). Gating strategies are shown in Supplementary Fig. 3B. Total RNA was isolated with the RNeasy$^®$ mini kit (QIAGEN), and cDNA was synthesized using the RevertAid$^{TM}$ First Strand cDNA Synthesis Kit (Thermo Fisher Scientific). Relative gene expression levels were measured by quantitative reverse transcription-polymerase chain reaction (RT-PCR) using Fast SYBR$^®$ Green Master Mix (Applied Biosystems) on a StepOnePlus$^{TM}$ system (Applied Biosystems) with the cycle threshold method. Donor and sample characteristics are provided in Supplementary Table 6, and primers are described in Supplementary Table 7.

## Microarray data analysis

RNA expression levels for *CXCR6* and *CXCL16* from laser-dissected tissue from mixed active/inactive and inactive demyelinated lesions were obtained from a microarray dataset (Hendrickx *et al.*, 2017). Adjusted *P*-values are shown in Fig. 5.

## Statistical analysis

All analyses were performed in GraphPad Prism 6 or 7 (GraphPad Software, San Diego, CA, USA). When data were not normally distributed non-parametric tests, either Kruskall-Wallis or Mann-Whitney U-tests were performed. Dunn's test was used for multiple comparisons. When data were normally distributed one-way ANOVA test was used together with Tukey *post hoc* test.

## Data availability

The data that support the findings of this study are available from the corresponding author, upon reasonable request.

# Results

## Multiple sclerosis normal-appearing white matter is enriched for T cells

We first quantified the presence of CD3$^+$ T cells in normal-appearing white matter of the pyramidal tract at the level of the medulla oblongata of multiple sclerosis, Alzheimer's disease, and non-neurological control brains (Fig. 1A). Donor and sample characteristics were comparable for all three groups (Table 1 and Supplementary Table 1). However, brain weight was significantly lower in the multiple sclerosis and Alzheimer's disease cases compared to the non-neurological controls, indicating brain tissue loss in the diseased brains (Supplementary Fig. 4). In multiple sclerosis brains, more T cells were encountered compared to Alzheimer's disease and control brains (Fig. 1B). We then assessed the relationship between the number of T cells and axonal loss in pyramidal tract normal-appearing white matter. Axon density was significantly reduced in the multiple sclerosis cases compared to the controls, indicating axonal loss in multiple sclerosis normal-appearing white matter (Fig. 1C). Axon density did not correlate with the number of T cells in multiple sclerosis normal-appearing white matter (Fig. 1D).

## Inflammatory active white matter lesions are enriched for CD4$^+$ and CD8$^+$ T cells

In sections of subcortical white matter of controls, Alzheimer's disease cases, and multiple sclerosis cases containing different lesion types, both lesional and perilesional white matter were delineated, and CD3$^+$ T cells were quantified (Supplementary Fig. 1). T cell counts in pyramidal tract and subcortical white matter were comparable for non-neurological controls; however, T cell counts were higher in (perilesional) subcortical white matter compared to the pyramidal white matter tract in both the multiple sclerosis and Alzheimer's disease cases (*cf.* Fig. 1B and E).

Perilesional white matter and all multiple sclerosis lesion types contained more T cells compared to control white matter, but were comparable to neurodegenerative control white matter. When compared to multiple sclerosis perilesional white matter, both active and mixed active/inactive lesions were enriched for CD3$^+$ T cells (Fig. 1E). This enrichment was observed both for CD4$^+$ and CD8$^+$ T cells (Fig. 1F and G), without a skewing of the CD8/CD4 ratio between lesion types (Supplementary Fig. 5A). Interestingly, the number of CD8$^+$ T cells was reduced in remyelinated areas (shadow plaques) compared to inflammatory active and mixed active/inactive lesions (Fig. 1G). Furthermore, the CD8/CD4 ratio was variable between donors, but consistent between the different regions of individual donors (Supplementary Fig. 5A and B). Interestingly, multiple sclerosis donors with a low CD8/CD4 ratio showed a higher percentage of inactive remyelinated areas in all dissected tissue blocks compared to donors with a high CD8/CD4 ratio (Supplementary Fig. 5C). Because CD8$^+$ T cells were, next to active lesions, also more closely associated with mixed active/inactive lesions, our further analysis focused on CD8$^+$ T cells.

## CD8$^+$ T cells are restricted to the PVS, except in inflammatory active and mixed active/inactive lesions

We next assessed the localization of CD8$^+$ T cells in multiple sclerosis normal-appearing white matter, mixed active/
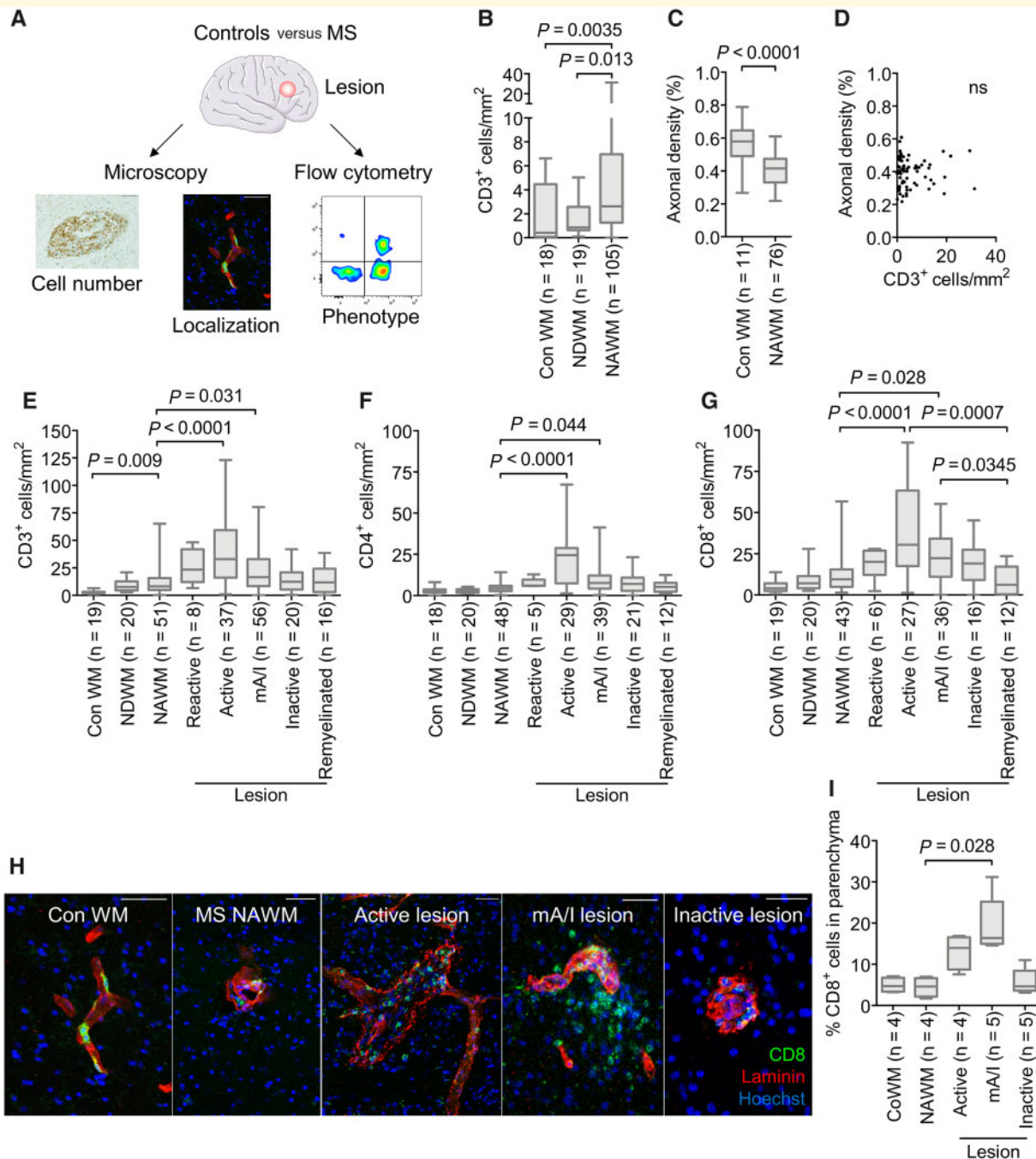
**Figure 1 T cell numbers are increased in multiple sclerosis normal-appearing white matter and further enhanced in inflammatory active and mixed active/inactive lesions.** (**A**) Illustration of experimental set-up. (**B**) Number of CD3$^+$ cells in the pyramid tract of non-neurological control (Con) white matter, Alzheimer's disease neurodegenerative white matter, and multiple sclerosis normal-appearing white matter at a standardly dissected location at the level of the medulla oblongata (Kruskall–Wallis test $P$ = 0.0002). (**C**) Axonal density in control white matter and multiple sclerosis normal-appearing white matter in the pyramid tract. (**D**) Correlation of axonal density with the number of T cells in multiple sclerosis normal-appearing white matter in the pyramid tract. (**E**) Number of CD3$^+$ cells in subcortical white matter lesions (Kruskall–Wallis test $P$ < 0.0001). (**F**) Number of CD4$^+$ cells in subcortical white matter lesions in active and mixed active/inactive lesions compared to normal-appearing white matter and remyelinated areas (Kruskall–Wallis test $P$ < 0.0001). (**G**) Number of CD8$^+$ cells in subcortical white matter in active and mixed active/inactive lesions compared to normal-appearing white matter (Kruskall–Wallis test $P$ < 0.0001). (**H**) Confocal images of CD8 and laminin immunofluorescent staining from control white matter, normal-appearing white matter, active lesion, mixed active/inactive lesion, and inactive lesion. Scale bars = 50 μm. (**I**) Percentage of CD8$^+$ cells located in brain parenchyma (Kruskall–Wallis test $P$ = 0.0042). Note that the quantification of control white matter CD8$^+$ cells in brain parenchyma has been published previously (Smolders *et al.*, 2018) and is shown here for comparison. Kruskall-Wallis and Dunn's *post hoc* test were used and $P$-values are shown in the plots. ConWM = control white matter; mA/I = mixed active/inactive; MS = multiple sclerosis; NAWM = normal-appearing white matter; NDWM = neurodegenerative white matter.

inactive lesions, and inactive lesions, by staining the laminin-gamma subunit in basement membranes. The PVS, the Virchow–Robin space, is the only compartment in the human body delineated by two basement membranes, covered on the luminal side by specialized endothelium and on the parenchymal side by the glia limitans (Sorokin, 2010). These basement membranes contain various matrix proteins, including different laminin chains and collagen type IV (van Horssen *et al.*, 2005). In multiple sclerosis normal-appearing white matter, CD8$^+$ T cells were found almost exclusively in the PVS, comparable to control white matter (Fig. 1H). In active and mixed active/inactive lesions, an increased proportion of CD8$^+$ T cells infiltrated the brain parenchyma (median 13.9% and 16.5%, respectively). In inactive lesions, the percentage of parenchymal CD8$^+$ T cells was comparable to the multiple sclerosis normal-appearing white matter (Fig. 1I).

## Progressive multiple sclerosis donors show perivascular cuffing of T cells

In the multiple sclerosis normal-appearing white matter, we occasionally observed large clusters of T cells restricted to the PVS, which were previously characterized as perivascular cuffs (Revesz, 1994). We systematically scored all medulla oblongata sections for the presence of perivascular T-cell cuffing (Fig. 2A). T cell cuffs were only encountered in the progressive multiple sclerosis donors (Fig. 2B). Interestingly, donors with perivascular cuffs showed a higher number of demyelinated lesions in the brainstem and a higher percentage of mixed active/inactive lesions (Fig. 2C and D). There were no significant differences in the percentage of remyelinated active lesions or the number of reactive sites in the brainstem and the total disease duration or time from first symptoms until the patient needed a walking aid (data not shown).

## Multiple sclerosis lesion T cells show a CD8$^+$ T$_{RM}$ cell surface marker profile

We next analysed rapidly-isolated post-mortem mononuclear cells for the expression of phenotypic markers that we recently identified on human brain T$_{RM}$ cells by flow cytometry (Smolders *et al.*, 2018). These included the canonical markers CD69 and CD103 (Szabo *et al.*, 2019), but also programmed death receptor 1 (PD-1), very late antigen-1 (VLA-1, CD49a), and the general memory marker CD44 (Kumar *et al.*, 2017). Cells were acquired from fresh multiple sclerosis tissue blocks containing either mixed active/inactive ($n = 3$) or active ($n = 5$) lesions, multiple sclerosis normal-appearing white matter ($n = 7$), and control white matter tissue ($n = 10$) (Fig. 3A, donor and sample information in Supplementary Table 4).
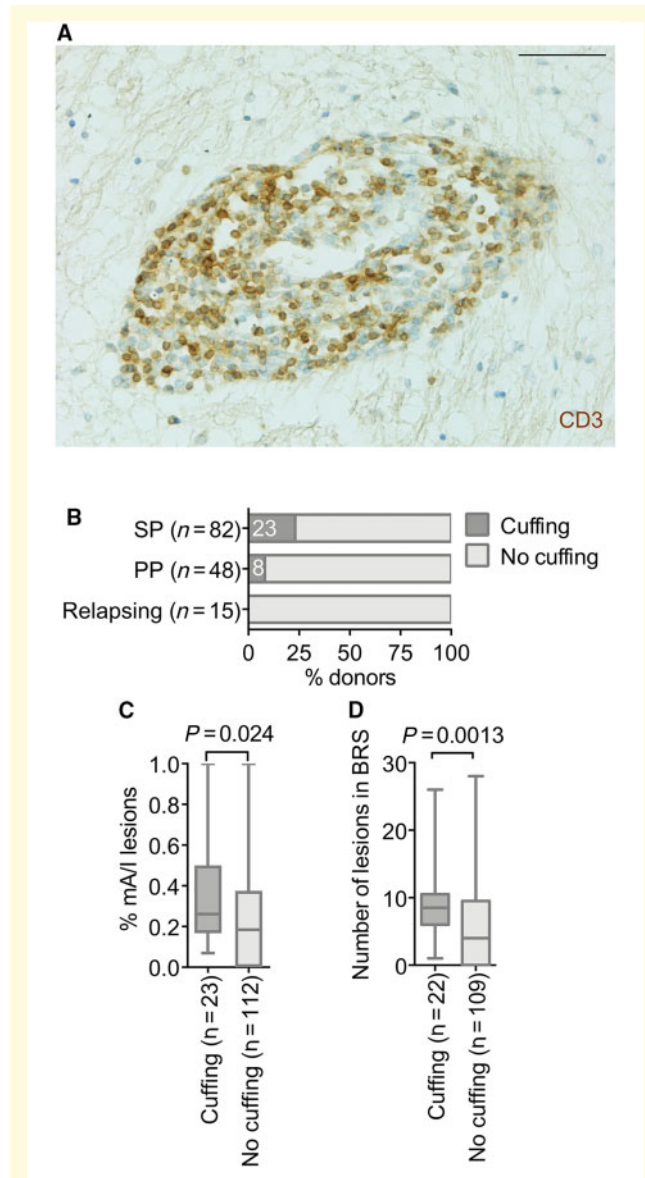


**Figure 2 Clinical and pathological correlates of perivascular cuffing of CD3$^+$ cells at a standardly dissected location at the level of the medulla oblongata.** (**A**) CD3$^+$ perivascular cuff showing more than one ring of CD3$^+$ cells around a blood vessel at the level of the medulla oblongata. Scale bar = 50 μm. (**B**) Multiple sclerosis cases with perivascular cuffing more often show a progressive multiple sclerosis disease course (chi-square test $P = 0.017$). (**C** and **D**) Multiple sclerosis cases with perivascular cuffing show a higher brainstem demyelinated lesion load (**C**) and a higher percentage of mixed active/inactive lesions (**D**). Mann-Whitney U-test was used, and $P$-values are shown in the plots. BRS = brainstem; mA/I = mixed active/inactive; PP = primary progressive; SP = secondary progressive.

Virtually all T cells isolated from multiple sclerosis lesions were CD69$^+$, with both a CD103$^+$ and a CD103$^-$ fraction present (Fig. 3B). There was a lower fraction of CD69$^-$CD103$^-$CD8$^+$ T cells in multiple sclerosis lesions compared to control white matter (Fig. 3C).

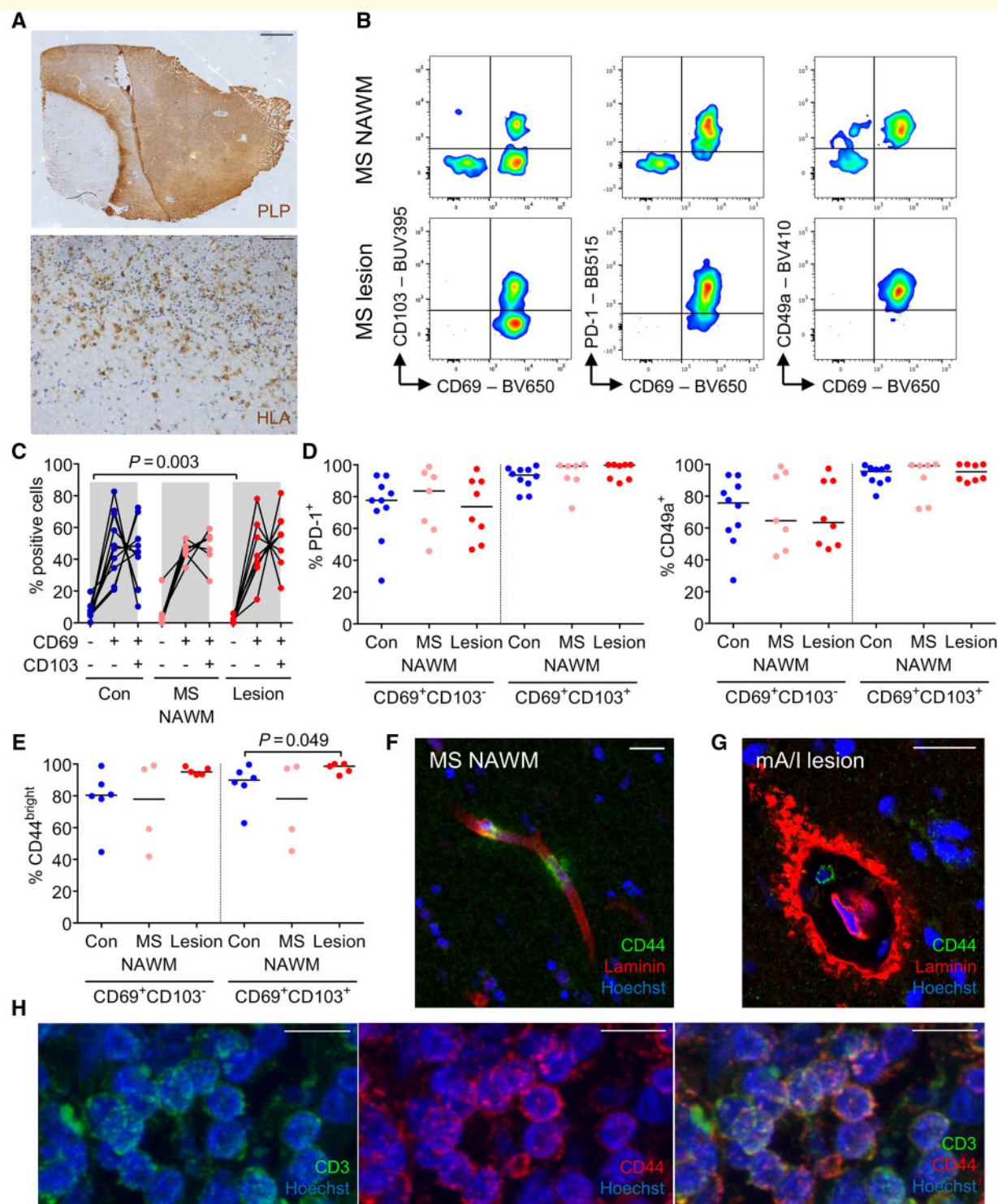**Figure 3 CD8+ T cells in multiple sclerosis lesions show a T_RM cell surface marker profile.** (A) An example of PLP and HLA staining of a multiple sclerosis mixed active/inactive lesion dissected for cell isolation. Scale bar = 1 mm (PLP) and 100 μm (HLA). (B) Flow-cytometric plots for CD103, CD69, PD-1, and CD49a expression on CD8+ T cells from multiple sclerosis normal-appearing white matter and lesions. (C) Percentage of single- and double-positive cells for CD69 and CD103 in control white matter, multiple sclerosis normal-appearing white matter, and multiple sclerosis lesions. (D) Percentage of PD-1+ and CD49a+ CD8+ T cells is comparable in control white matter, multiple sclerosis normal-appearing white matter, and multiple sclerosis lesions. PD-1 and CD49a expression is increased in CD103+ cells. (E) Multiple sclerosis normal-appearing white matter and multiple sclerosis lesion CD8+ T_RM cells are CD44bright. (F) In the PVS of multiple sclerosis normal-appearing white matter, CD44+ T cells are located in close contact to the CD44 ligand, laminin. Scale bar = 25 μm. (G) In the inactive centre of mixed active/inactive lesions, CD44+ T cells are present in the PVS. The basal lamina in inactive centres appears fibrotic. Scale bar = 25 μm. (H) T cell clusters in multiple sclerosis perivascular cuffs show high CD44 expression. Scale bar = 10 μm. Con = control; mA/I = mixed active/inactive; MS = multiple sclerosis; NAWM = normal-appearing white matter; NDWM = neurodegenerative white matter.

Because the presence of CD103 impacts on the phenotype of brain $T_{RM}$ cells (Wakim *et al.*, 2012; Smolders *et al.*, 2018), we stratified further analyses for expression of CD103. Expression of the $T_{RM}$ markers PD-1, CD49a, and CD44 was equally high on CD8$^+$ T cells from all three categories of tissue subtypes sampled (Fig. 3B, D and E). Interestingly, CD49a is a receptor for collagen type IV and CD44 can act as a receptor for laminin, among others, and both molecules may hereby modulate homing of brain $T_{RM}$ cells in the PVS (Topham and Reilly, 2018). CD44$^+$ lymphocytes could also be observed in close contact with laminin in the PVS with immunohistochemistry in both normal-appearing white matter and inactive centres of multiple sclerosis lesions (Fig. 3F and G). Perivascular T cell clusters showed high expression of CD44 (Fig. 3H).

## Circulating T cells are almost absent in chronic multiple sclerosis autopsy lesions

Next we compared the presence of S1P1$^+$ circulating T cells and the CD103$^+$ $T_{RM}$ cell subset in both inflammatory active lesions from early multiple sclerosis biopsy cases and chronic progressive multiple sclerosis autopsy cases. In both lesion stages, we encountered CD103$^+$ $T_{RM}$ cells in the brain parenchyma (Fig. 4A). In the early multiple sclerosis lesion stages, a relatively smaller proportion of CD3$^+$ T cells was CD103$^+$ compared to the chronic progressive multiple sclerosis autopsy cases (Fig. 4B), which suggests a smaller pool of CD103$^+$ $T_{RM}$ cells in early multiple sclerosis lesions. We stained for the recirculation marker S1P1 and found, in accordance with earlier studies (Van Doorn *et al.*, 2010; Brana *et al.*, 2014; Machado-Santos *et al.*, 2018), no staining of S1P1$^+$ T cells in the parenchyma or PVS of biopsy or autopsy material. Almost all S1P1$^+$ cells in biopsy samples were located directly adjacent to the luminal side of the endothelium (Fig. 4C). However, where few intravascular S1P1$^+$ T cells were found in inflammatory active lesions from chronic progressive multiple sclerosis autopsy, they were present at high number in lesions from early multiple sclerosis biopsies (Fig. 4C and D). Although a post-mortem effect cannot be excluded, desensitization of S1P1 is an important mechanism for effector T cells to migrate from the circulation into tissues (Arnon *et al.*, 2011). Close contact with the endothelium suggests that T cells in early multiple sclerosis biopsies may reflect an expanded local pool of intravascular effector-type T cells, which may lose S1P1 upon infiltration of the PVS. This interpretation would support a role for non-$T_{RM}$ cells in early multiple sclerosis, which was not observed in end-stage multiple sclerosis.

## T-SNE analysis identifies exclusively CD8$^+$ $T_{RM}$ cell clusters in multiple sclerosis cases

To evaluate the presence of small T cell clusters lacking a $T_{RM}$ cell phenotype in lesions, which may get lost in conventional gating strategies, we generated t-SNE plots of the total CD3$^+$CD8$^+$ T cell fraction. Only in the control donors, unique clusters of cells displaying a non-$T_{RM}$ cell phenotype were encountered, characterized by a lack of CD69 expression (Fig. 5A, clusters 1 and 2). These cells showed low expression of $T_{RM}$ cell surface markers and, in cluster 2, high expression of molecules related to cytotoxicity (granzyme B and GPR56). In multiple sclerosis normal-appearing white matter and lesions, dominant T-cell clusters showed a $T_{RM}$ cell phenotypic profile with clusters 5 and 9 being characterized by high expression of CD103.

## CD8$^+$ $T_{RM}$ cells in multiple sclerosis lesions upregulate the tissue homing receptor CXCR6

CXCR6 is a core $T_{RM}$ cell marker and a chemokine receptor mediating tissue infiltration of CD8$^+$ T cells (Kumar *et al.*, 2017). The percentage of CXCR6$^+$ CD8$^+$ T cells was increased in multiple sclerosis lesions compared to control white matter in both the CD103$^+$ and CD103$^-$ CD8$^+$ T-cell population (Fig. 5B and C). In addition, whole tissue gene expression microarray analysis of laser-dissected control white matter as well as mixed active/inactive and inactive multiple sclerosis lesions (Hendrickx *et al.*, 2017) revealed increased expression of CXCR6 in the rim of mixed active/inactive lesions (Fig. 5D). The ligand of CXCR6, CXCL16, is also upregulated in the rim of mixed active/inactive lesions, indicated by quantitative RT-PCR (Hendrickx *et al.*, 2013) and by microarray analysis (Fig. 5D). CXCR6–CXCL16 interaction may mediate homing of CD8$^+$ T cells in the inflamed parenchyma because these are found in the inflammatory active rim of mixed active/inactive lesions in close contact to CXCL16$^+$ cells [median (interquartile range, IQR) 42.8% (34.9–43.9%) of parenchymal T cells; $n = 3$] (Fig. 5E and F).

## Lesional CD8$^+$ $T_{RM}$ cells show signs of reactivation without notable cytotoxicity

To assess the activation status of brain $T_{RM}$ cells, we stained for Ki-67. Ki-67 is a marker for T cells undergoing antigen-specific proliferation *in vitro* (Soares *et al.*, 2010). In cells isolated from lesions, higher expression of Ki-67, as measured by the geometric mean fluorescence intensity (GMFI), was observed when compared to control white matter with flow cytometry (Fig. 6A and B), which can indicate an increased rate of recent reactivation. The T-cell clusters in the PVS contained CD3$^+$ T cells positive for Ki-67 with immunohistochemistry (Fig. 6C and D).

Next, we analysed expression of the cytotoxic enzyme granzyme B, which was earlier observed with immunohistochemistry in CD8$^+$ T cells in active lesions (van Nierop *et al.*, 2017; Machado-Santos *et al.*, 2018). Using immunohistochemical staining, we encountered low numbers of
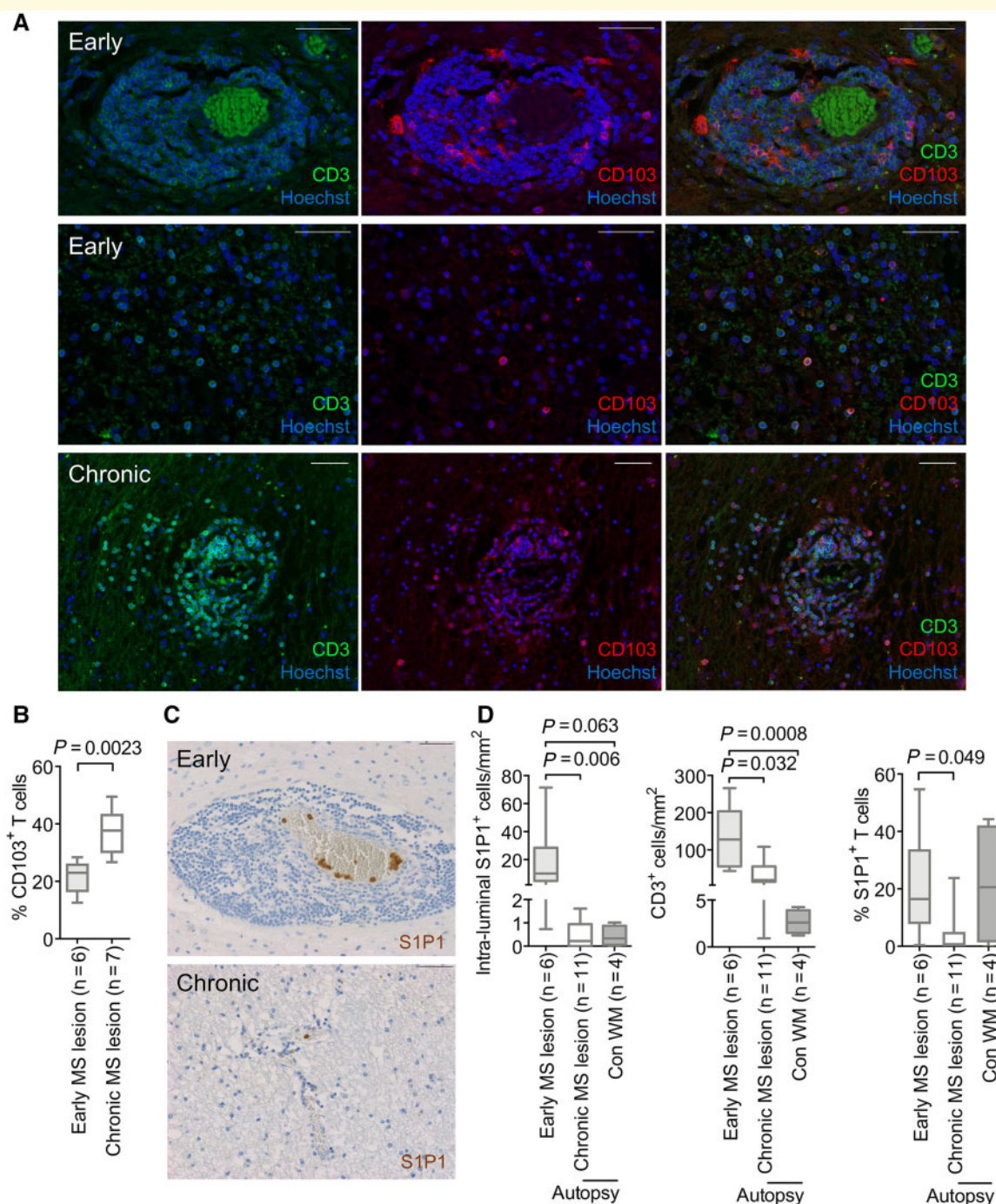
**Figure 4 CD103$^+$ T cells infiltrate the brain parenchyma in early biopsy and chronic autopsy multiple sclerosis lesions, while circulating S1P1$^+$ T cells are almost absent in chronic autopsy cases.** (**A**) Confocal images of CD3 and CD103 immunofluorescent staining showing CD103$^+$ T cells in both the PVS and the brain parenchyma in both early and chronic multiple sclerosis lesions. The bright green signal inside the blood vessel lumen is autofluorescence from erythrocytes. Scale bars = 50 μm. (**B**) The percentage of CD103$^+$ T cells was increased in chronic multiple sclerosis lesions (Mann-Whitney U-test P = 0.0023) (**C**) S1P1$^+$ are present mostly in early multiple sclerosis lesions and located within the blood vessel lumen, confirming these are circulating T cells. Scale bars = 50 μm. (**D**) The absolute number of S1P1$^+$ cells in blood vessels is decreased in chronic multiple sclerosis autopsy lesions compared to early multiple sclerosis biopsy lesions that are both inflammatory active (Kruskall–Wallis test P = 0.0017). The total number of T cells was decreased in chronic multiple sclerosis lesions compared to early multiple sclerosis lesions (Kruskall-Wallis test P = 0.0001). The relative number of S1P1$^+$ T cells was lower in chronic multiple sclerosis lesions compared to early multiple sclerosis lesions (Kruskall-Wallis test P = 0.049). Dunn's *post hoc* test was used and P-values are shown in the plots. Con WM = control white matter; MS = multiple sclerosis.
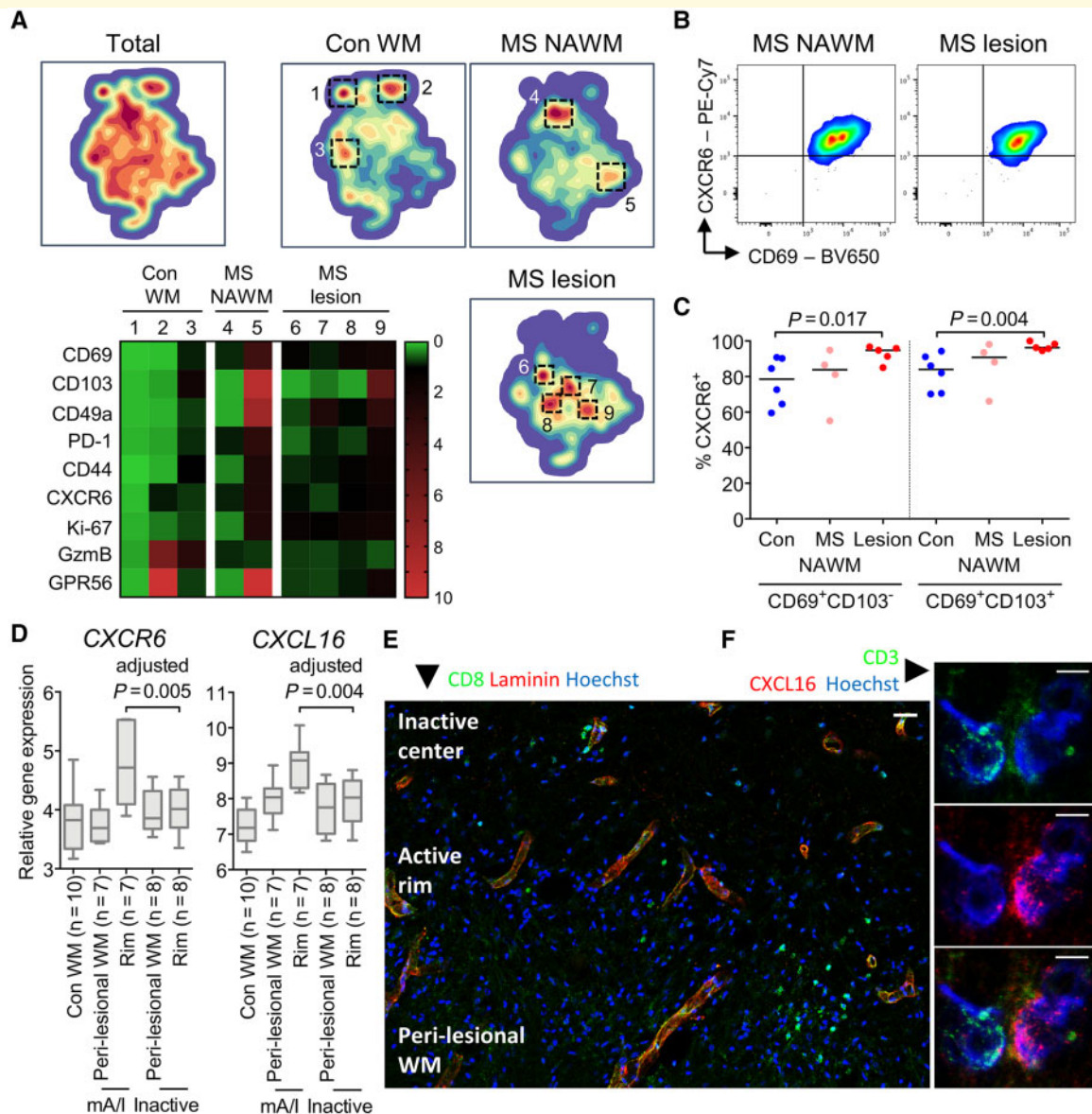
**Figure 5 Multiple sclerosis normal-appearing white matter and multiple sclerosis lesions show a distinct $T_{RM}$ cell surface marker profile with a higher percentage of CXCR6$^+$ CD8$^+$ T cells in multiple sclerosis lesions.** (**A**) T-SNE analysis of all CD3$^+$CD8$^+$ T cells reveals distinct cell clusters in control white matter, multiple sclerosis normal-appearing white matter, and multiple sclerosis lesions. The heat map shows the expression pattern in the indicated T cell clusters. (**B**) Flow cytometric plots for CXCR6 and CD69 expression on CD8$^+$ $T_{RM}$ cells in control white matter, normal-appearing white matter, and multiple sclerosis lesion samples. (**C**) CXCR6 is upregulated in multiple sclerosis lesions in both CD103$^-$ and CD103$^+$ cells (Kruskall-Wallis test $P = 0.0357$). (**D**) Tissue mRNA gene expression levels from mixed active/inactive lesions shows upregulation of *CXCR6* and its ligand, *CXCL16*. (**E**) CD8$^+$ T cells are found in brain parenchyma in the mixed active/inactive lesion rim. Scale bar = 50 μm. (**F**) CD3$^+$ T cells in close contact to a CXCL16$^+$ cell in an inflammatory active multiple sclerosis lesions. Scale bar = 5 μm. Mann-Whitney U- and Kruskall-Wallis tests were used, and (adjusted) *P*-values are shown in the plots. Con WM = cnotrol white matter; mA/I = mixed active/inactive; MS = multiple sclerosis; NAWM = normal-appearing white matter.

granzyme B$^+$ cells in inflammatory active multiple sclerosis lesions [median (IQR) = 0.017 (0.012–0.026) per mm$^2$ in 12 tissue sections containing inflammatory active multiple sclerosis lesions; Fig. 6E], while these tissue sections contained high numbers of CD3$^+$ cells [median (IQR) = 36.9 (11.1–39.6) per mm$^2$]. We observed with flow cytometry equally low numbers of granzyme B$^+$ CD8$^+$ T cells in

fractions from control white matter and multiple sclerosis normal-appearing white matter and lesions (Fig. 6F). In accordance with earlier data, lowest granzyme B expression was observed in the CD103$^+$ $T_{RM}$ cell subset (Smolders *et al.*, 2018). Therefore, our data do not support an upregulation of granzyme B as cytotoxic effector molecule by lesional $T_{RM}$ cells.
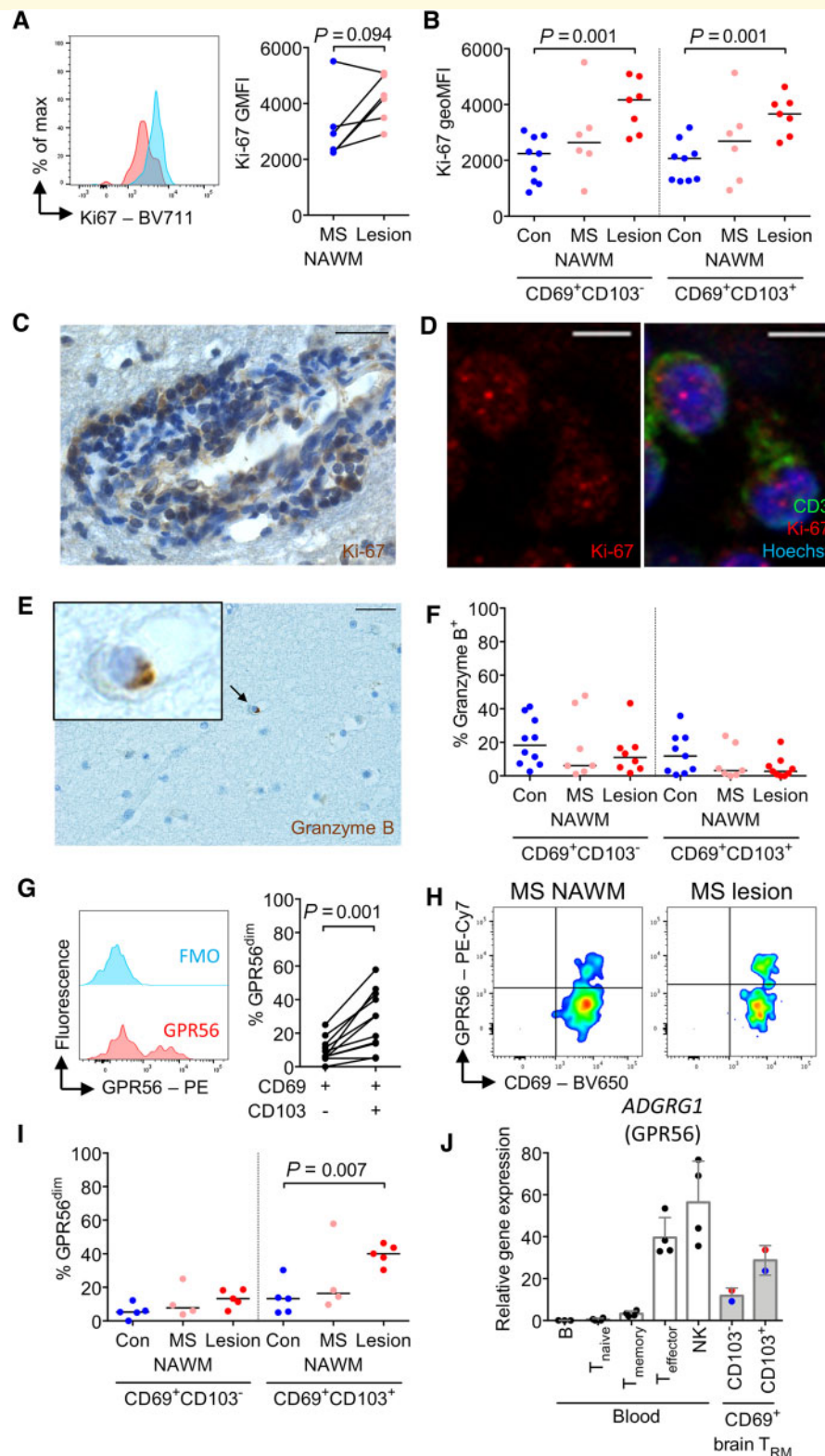
**Figure 6 CD8$^+$ T$_{RM}$ cells in multiple sclerosis lesions are reactivated and show increased expression of GPR56 without upregulation of granzyme B.** (**A**) Ki-67 signal in CD8$^+$ T$_{RM}$ cells from multiple sclerosis normal-appearing white matter and multiple sclerosis lesions. (**B**) In multiple sclerosis lesion CD8$^+$ T$_{RM}$ cells upregulate Ki-67 expression compared to controls, both in CD103$^+$ and CD103$^-$ T$_{RM}$ cells (Kruskall-Wallis test $P = 0.0081$). (**C**) T cells within perivascular cuffs are Ki-67$^+$. Scale bar = 25 μm. (**D**) Expression of nuclear Ki-67 in CD3$^+$ T cells. Scale bar = 5 μm. (**E**) Immunohistochemistry of a granzyme B$^+$ cell in a subcortical white matter multiple sclerosis lesion. Scale bar = 25 μm. (**F**) There is no difference in the percentage of granzyme B$^+$ cells derived from multiple sclerosis lesions compared to control white matter. (**G**) Brain T$_{RM}$ cells show GPR56$^{dim}$ expression, with a higher percentage of positive cells in CD103$^+$ compared to CD103$^-$ T$_{RM}$ populations.

(continued)

The adhesion G protein-coupled receptor GPR56 is expressed at high levels on circulating cytotoxic lymphocytes, where it inhibits immediate effector functions (Chang *et al.*, 2016). Previously, we found almost no GPR56^{high} expression on CD8^{+} brain $T_{RM}$ cells (Smolders *et al.*, 2018). In multiple sclerosis lesions, we saw an expansion of a GPR56^{dim} subset in the CD8^{+}CD69^{+}CD103^{+} $T_{RM}$ cell fraction (Fig. 6G–I). This CD103^{+} cell-restricted expansion was confirmed by quantitative RT-PCR (Fig. 6J). Expression of GPR56 may reflect cytotoxic capacity of multiple sclerosis lesion brain $T_{RM}$ cells but may also restrict granzyme B expression.

## Perivascular cuffs show signs of $T_{RM}$ cell reactivation

In search for the site of $T_{RM}$ cell reactivation, we stained the perivascular cuffs for antigen presentation and reactivation markers. As shown above, Ki-67^{+} CD3^{+} T cells were observed in these clusters (Fig. 6C and D), suggesting that reactivation could occur in these perivascular cuffs. Within the perivascular T cell cuffs, large populations of CD3^{+}CD103^{+} $T_{RM}$ cells were observed (Fig. 7A). A median proportion of 73.1% (IQR 64.7–84.6%) of these $T_{RM}$ cells showed expression of E-cadherin, the ligand for CD103, which may be involved in clustering of these cells (Topham and Reilly, 2018) (Fig. 7B; *n* = 3). In the perivascular cuffs, we found CD103^{+} $T_{RM}$ cells in close proximity to HLA^{+} (Fig. 7C and D) and CD163^{+} (Fig. 7E) perivascular macrophages and CD20^{+} B cells (Fig. 7F), which could both be involved in antigen presentation and reactivation of $T_{RM}$ cells within the PVS in chronic multiple sclerosis cases and accumulating in mixed active/inactive lesions.

## Discussion

Here we provide an extensive analysis of the phenotypic profile and spatial localization of human brain T cells in relation to the post-mortem pathology of advanced multiple sclerosis. We show that the number of T cells is increased in multiple sclerosis normal-appearing white matter and is enhanced further in inflammatory active multiple sclerosis white matter lesions. In line with previous reports (Smolders *et al.*, 2013, 2018; van Nierop *et al.*, 2017; Machado-Santos *et al.*, 2018), we show that these are mostly CD8^{+} $T_{RM}$

cells, which lack characteristics of circulating lymphocytes. We expand previous work by elaborating on the phenotypic and functional profile of these cells and associating their characteristics with the localization in the PVS. In multiple sclerosis normal-appearing white matter, CD8^{+} $T_{RM}$ cells were retained in the PVS, likely mediated by high expression of CD44 and CD49a. We found that clustering of CD8^{+} $T_{RM}$ cells in perivascular cuffs is only observed in donors with progressive multiple sclerosis. In mixed active/inactive lesions, CD8^{+} $T_{RM}$ cells also localized in the brain parenchyma. This is possibly mediated by high expression of the tissue homing receptor CXCR6 by lesional CD8^{+} $T_{RM}$ cells, since its ligand CXCL16 also shows increased expression in the mixed active/inactive lesion rim. CD8^{+} $T_{RM}$ cells in multiple sclerosis lesions showed a higher expression of Ki-67, presumably reflecting recent reactivation. We observed antigen-presenting cells in conjunction with Ki-67^{+} $T_{RM}$ cells in the perivascular cuffs, suggesting that these are potential hotspots of this reactivation. We further observed a low expression of granzyme B, which could be due to the high expression of inhibitory GPR56. The quantities, localization, and activation state of these cells, together with the association of perivascular T cell clusters with lesion load, mixed active/inactive lesions, and progressive disease, suggest that reactivation of CD8^{+} $T_{RM}$ cells in the PVS is a key mechanism in the maintenance of white matter lesion activity in advanced progressive multiple sclerosis.

Only in demyelinated white matter lesions did we observe substantial numbers of CD8^{+} $T_{RM}$ cells outside the PVS. Generating cytotoxic mediators, such as granzyme B, is an effector mechanism of reactivated $T_{RM}$ cells (Mueller and Mackay, 2016). Surprisingly, we did not find an enrichment of granzyme B^{+} cells in the cell fraction isolated from lesions. This finding contrasts with an enrichment for granzyme B^{+} T cells in multiple sclerosis lesions reported by Van Nierop *et al.* (2017). A sampling error is unlikely as only few granzyme B^{+} cells were stained with immunohistochemistry in lesions as well. This does not suggest an upregulation of the granzyme B–perforin axis in chronic multiple sclerosis lesions as was observed in early multiple sclerosis diagnostic biopsy samples (Konjevic Sabolek *et al.*, 2019). In general, brain CD103^{+} $T_{RM}$ cells show low expression of granzyme B and are almost devoid of perforin (Smolders *et al.*, 2013, 2018). One of the reasons for this lack of cytotoxicity could be the expression of intermediate levels of GPR56 by multiple sclerosis lesional CD103^{+} $T_{RM}$ cells. GPR56 is

**Figure 6** Continued

**(H)** Some multiple sclerosis normal-appearing white matter and multiple sclerosis lesion $T_{RM}$ cells show GPR56^{dim} expression. **(I)** The percentage of GPR56^{dim} cells is increased in CD69^{+}CD103^{+} CD8^{+} $T_{RM}$ cells derived from multiple sclerosis lesions compared to control white matter. **(J)** Relative gene expression for *ADGRG1* (GPR56) in FACS-sorted CD20^{+} B cells, naïve, memory, effector CD8^{+} T cells, and NK cells from peripheral blood and CD103^{−} and CD103^{+} CD69^{+}CD8^{+} $T_{RM}$ cells from brain samples showing increased *ADGRG1* expression in CD103^{+} cells. Sample 1 (blue circles) and sample 2 (red circles) were pooled cells from derived from five and three donors, respectively. Mann-Whitney U-test was used, and *P*-values are shown in the plots. Con = control; GMFI = geometric mean fluorescence intensity; MS = multiple sclerosis; NAWM = normal-appearing white matter.
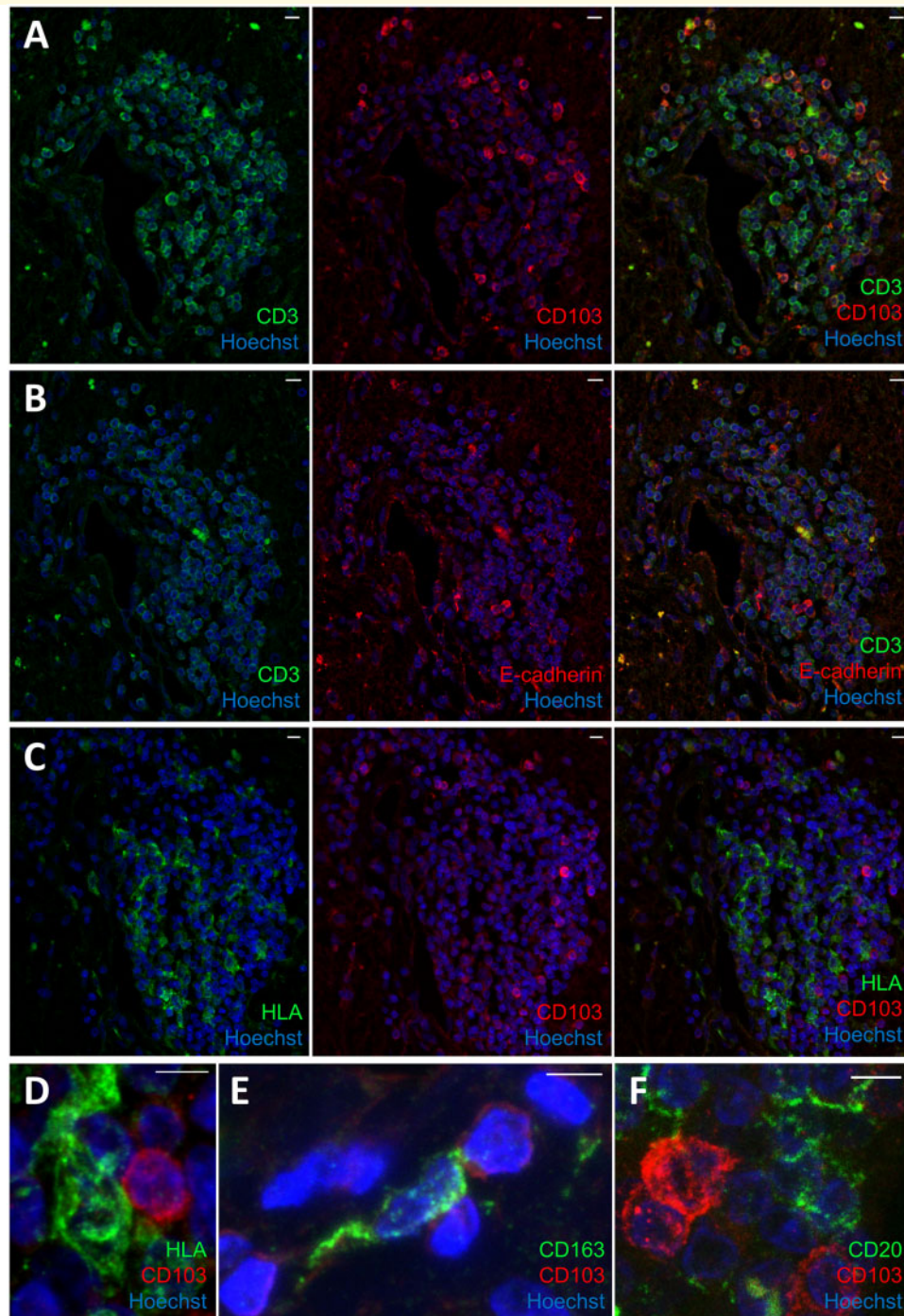
**Figure 7 Perivascular cuffs consist of CD103$^+$ T$_{RM}$ cells in close contact with perivascular macrophages and B cells suggesting antigen presentation and reactivation of T$_{RM}$ cells in the perivascular space.** (**A**) CD3$^+$ T cells in perivascular clusters express CD103. (**B**) CD3$^+$ T cells in perivascular clusters express the ligand for CD103, E-cadherin. (**C**) HLA$^+$ perivascular macrophages are present in perivascular cuffs. (**D–F**) In perivascular cuffs, CD103$^+$ T$_{RM}$ cells are found in close proximity to HLA$^+$ and CD163$^+$ perivascular macrophages (**D** and **E**) and to CD20$^+$ B cells (**F**). Scale bars = 10 μm in **A–C** and 5 μm in **D–F**.

expressed at high levels on circulating lymphocytes with cytotoxic capacities, where it inhibits effector functions (Chang *et al.*, 2016). In normal white matter, human post-mortem CD8$^+$ T$_{RM}$ cells produce more granzyme K than granzyme B (Smolders *et al.*, 2013, 2018), which could also

serve as an effector molecule in multiple sclerosis lesions. Furthermore, CD8$^+$ T$_{RM}$ cells express high levels of the inhibitory receptor PD-1. Previously, we observed expression of its ligand, programmed death-ligand 1 (PD-L1), in multiple sclerosis lesions but not in control white matter

(Smolders *et al.*, 2018). In polyomavirus-infected mice, expression of PD-L1 was observed on myeloid cells, microglia, and astrocytes (Shwetank *et al.*, 2019). Conversely, blockade of the PD-1 system in treatment of human melanoma patients with immune checkpoint inhibitors has been associated with the occurrence of multiple sclerosis-like demyelinating lesions (Maurice *et al.*, 2015; Durães *et al.*, 2018). Cytokine production by activated CD8$^+$ T$_{RM}$ cells could contribute to the maintenance of mixed active/inactive lesions. Human white matter CD8$^+$ T$_{RM}$ cells are potent producers of IFNγ, granulocyte-macrophage colony-stimulating factor, and tumour necrosis factor upon activation (Smolders *et al.*, 2018). Also, Fas ligand-mediated killing of Fas-expressing oligodendrocytes around multiple sclerosis lesions could be a potential mechanism by which CD8$^+$ T cells contribute to demyelination in chronic multiple sclerosis lesions (D'Souza *et al.*, 1996; van Nierop *et al.*, 2017; Fransen *et al.*, 2019; Wagner *et al.*, 2020).

In multiple sclerosis normal-appearing white matter, CD8$^+$ T$_{RM}$ cells were observed in their normal compartment, the PVS. Within this compartment, accumulation of inflammatory cells in perivascular cuffs has since long been recognized as an important pathological feature of multiple sclerosis (Prineas and Wright, 1978). In our dataset, perivascular cuffing at the medulla oblongata was only observed in progressive multiple sclerosis. Earlier studies found perivascular cuffing to be more prevalent in brain donors with secondary progressive multiple sclerosis compared to primary progressive multiple sclerosis (Revesz *et al.*, 1994). We now show these cuffs to contain T cells expressing the T$_{RM}$ cell marker CD103. Gray *et al.* earlier argued that T$_{RM}$ cell clustering with antigen-presenting cells, CD163$^+$ perivascular macrophages and B cells, could be the first step of ectopic lymphoid structure formation found in several inflammatory diseases (Gray *et al.*, 2018). In post-mortem multiple sclerosis studies, ectopic lymphoid structures are prevalent in the meninges of progressive donors (Serafini *et al.*, 2004; Haider *et al.*, 2016; Machado-Santos *et al.*, 2018) and may reflect mechanisms similarly to the role of perivascular cuffing. This idea is further supported by studies that show that the PVS and the meningeal compartment are connected (Dendrou *et al.*, 2015; Louveau *et al.*, 2015, 2016).

There are some limitations to our work. First, cells were isolated from tissue blocks containing both multiple sclerosis normal-appearing white matter and multiple sclerosis lesions, which may dilute differences in T cell phenotypes between both locations. As we did not use enzymes during the isolation procedure, we likely isolated only a proportion of cells from the brain tissue but on the other hand did not skew phenotypes by enzymatic digestion. Earlier studies showed that isolation procedures target subsets of tissue-resident cells and create skewing in phenotypes found (Steinert *et al.*, 2015). These aspects are covered by the combination with immunohistochemistry to validate our findings. Last, the overall numbers of cells sampled from tissue blocks are quite low, when compared to flow cytometric studies on peripheral blood mononuclear cells. This did not allow

sequencing of the brain T$_{RM}$ cell transcriptome. In particular, the number of CD4$^+$ T cells we isolated for flow cytometry studies was relatively low for reliable assessment. Strengths of our work are the well-characterized donor cohort and lesions, the combination of flow cytometry and immunohistochemistry, and the sample size.

Interestingly, in subcortical white matter from neurodegenerative controls we observed a comparable number of T cells compared to multiple sclerosis cases. This finding may relate to the lower weight of the Alzheimer's disease brains and/or the neurodegenerative process and is in line with two earlier reports on T cell numbers in relation to Alzheimer's disease pathology (Zotova *et al.*, 2013; Merlini *et al.*, 2018). It would be interesting to study differences in effector functions in Alzheimer's disease-associated T$_{RM}$ cells potentially involved in a neuroinflammatory response in neurodegenerative diseases. However, our data suggest that in advanced multiple sclerosis cases, the T$_{RM}$ cell response in normal-appearing white matter is not solely part of a neuroinflammatory response to the axonal damage, since we did not find a correlation with axonal density.

Furthermore, genetic risk factors for multiple sclerosis in immune-related genes (Attfield *et al.*, 2012; Dendrou *et al.*, 2015), effectiveness of therapies directed at circulating lymphocytes in the earlier stage of the disease (Wingerchuk and Weinshenker, 2016), and pathological features of chronic multiple sclerosis, like the lymphocytic infiltrates found in both PVS and meninges that mimic other immune-mediated diseases (Corsiero *et al.*, 2016), all lead us to think of multiple sclerosis as a primary immune-mediated disease. Therefore, a main open question is which antigen is presented to the CD8$^+$ T$_{RM}$ cells in the PVS of these chronic progressive multiple sclerosis brain donors. In other human and animal tissues investigated, T$_{RM}$ cell populations appear to control local viral infections (Szabo *et al.*, 2019). In models of CNS neurotropic virus infection, local brain CD8$^+$ T$_{RM}$ cell populations are generated against vesicular stomatitis virus (Wakim *et al.*, 2010), mouse polyomavirus (Shwetank *et al.*, 2019), West Nile virus (Aguilar-Valenzuela *et al.*, 2018), and non-replicating adenoviruses (Schøller *et al.*, 2019). This supports an antiviral response as a potential driver of CD8$^+$ T$_{RM}$ cell recruitment in the CNS, which may also be applicable to multiple sclerosis lesions. In a mouse model for multiple sclerosis, it was recently shown that viral infections during early life precipitate brain auto-immune disease by an increased recruitment of T$_{RM}$ cells into the brain (Steinbach *et al.*, 2019). In accordance, electron microscopy studies showed paramyxovirus-like fuzzy filament in nuclei of lymphocytes and macrophages in multiple sclerosis perivascular cuffs (Tanaka *et al.*, 1975), which could reflect the initiation of an antiviral T-cell response (Prineas, 1972). Identification of the exact cells expressing viral antigens and provoking subsequent CD8$^+$ T$_{RM}$ cell expansion could provide a critical avenue towards understanding the cause of multiple sclerosis. However, as low numbers of perivascular CD8$^+$ T$_{RM}$ cells are also observed in donors without multiple sclerosis (Smolders *et al.*, 2018), the

antigen presented to $T_{RM}$ cells in multiple sclerosis could be present both in donors with and without multiple sclerosis. Differences in genetic and environmental background could—in this scenario—accumulate in the destructive immune response seen in multiple sclerosis.

Altogether, our findings point to the PVS as a new frontier for progressive multiple sclerosis treatment development. Understanding the mechanisms that are involved in CD8$^+$ $T_{RM}$ cells expanding in the PVS, entering mixed active/inactive lesions, and driving ongoing inflammatory lesion activity could provide targets for new disease-modifying therapies with efficacy in progressive multiple sclerosis.

# Competing interests

The authors report no competing interests. I.H. received lecture and/or consultancy fee from Biogen and Novartis. J.S. received lecture and/or consultancy fee from Biogen, Merck, Novartis, and Sanofi-Genzyme.

# Supplementary material

Supplementary material is available at *Brain* online.

# References

Aguilar-Valenzuela R, Netland J, Seo Y-J, Bevan MJ, Grakoui A, Suthar MS. Dynamics of tissue-specific CD8 $^+$ T cell responses during West Nile virus infection. J Virol 2018; 92: e00014–18.

Arnon TI, Xu Y, Lo C, Pham T, An J, Coughlin S, et al. GRK2-dependent S1PR1 desensitization is required for lymphocytes to overcome their attraction to blood. Science 2011; 333: 1898–903.

Attfield KE, Dendrou CA, Fugger L. Bridging the gap from genetic association to functional understanding: the next generation of mouse models of multiple sclerosis. Immunol Rev 2012; 248: 10–22.

Babbe H, Roers A, Waisman A, Lassmann H, Goebels N, Hohlfeld R, et al. Clonal expansions of Cd8 $^+$ T cells dominate the T cell infiltrate in active multiple sclerosis lesions as shown by micromanipulation and single cell polymerase chain reaction. J Exp Med 2000; 192: 393–404.

Booss J, Esiri MM, Tourtellotte WW, Mason DY. Immunohistological analysis of T lymphocyte subsets in the central nervous system in chronic progressive multiple sclerosis. J Neurol Sci 1983; 62: 219–32.

Brana C, Frossard MJ, Pescini Gobert R, Martinier N, Boschert U, Seabrook TJ. Immunohistochemical detection of sphingosine-1-phosphate receptor 1 and 5 in human multiple sclerosis lesions. Neuropathol Appl Neurobiol 2014; 40: 564–78.

Chang G-W, Hsiao C-C, Peng Y-M, Vieira Braga FA, Kragten NAM, Remmerswaal EBM, et al. The adhesion G protein-coupled receptor GPR56/ADGRG1 is an inhibitory receptor on human NK cells. Cell Rep 2016; 15: 1757–70.

Corsiero E, Nerviani A, Bombardieri M, Pitzalis C. Ectopic lymphoid structures: powerhouse of autoimmunity. Front Immunol 2016; 7: 430.

Cossarizza A, Chang H-D, Radbruch A, Akdis M, Andrä I, Annunziato F, et al. Guidelines for the use of flow cytometry and cell sorting in immunological studies. Eur J Immunol 2017; 47: 1584–797.

D'Souza SD, Bonetti B, Balasingam V, Cashman NR, Barker PA, Troutt AB, et al. Multiple sclerosis: Fas signaling in oligodendrocyte cell death. J Exp Med 1996; 184: 2361–70.

Dendrou CA, Fugger L, Friese MA. Immunopathology of multiple sclerosis. Nat Rev Immunol 2015; 15: 545–58.

Van Doorn R, Van Horssen J, Verzijl D, Witte M, Ronken E, Van Het Hof B, et al. Sphingosine 1-phosphate receptor 1 and 3 are upregulated in multiple sclerosis lesions. Glia 2010; 58: 1465–76.

Downey GP, Doherty DE, Schwab B, Elson EL, Henson PM, Worthen GS. Retention of leukocytes in capillaries: role of cell size and deformability. J Appl Physiol 1990; 69: 1767–78.

Durães J, Coutinho I, Mariano A, Geraldo A, Macário MC. Demyelinating disease of the central nervous system associated with Pembrolizumab treatment for metastatic melanoma. Mult Scler J 2018; 135245851880372.

Fransen NL, Crusius JBA, Smolders J, Mizee MR, Eden CG, Luchetti S, et al. Post-mortem multiple sclerosis lesion pathology is influenced by single nucleotide polymorphisms. Brain Pathol 2019; 30: 106–19.

Frischer JM, Bramow S, Dal-Bianco A, Lucchinetti CF, Rauschka H, Schmidbauer M, et al. The relation between inflammation and neurodegeneration in multiple sclerosis brains. Brain 2009; 132: 1175–89.

Gray JI, Westerhof LM, MacLeod M. The roles of resident, central and effector memory CD4 T-cells in protective immunity following infection or vaccination. Immunology 2018; 154: 574.

Haider L, Zrzavy T, Hametner S, Höftberger R, Bagnato F, Grabner G, et al. The topograpy of demyelination and neurodegeneration in the multiple sclerosis brain. Brain 2016; 139: 807–15.

Hayashi T, Morimoto C, Burks JS, Kerr C, Hauser SL. Dual-label immunocytochemistry of the active multiple sclerosis lesion: major histocompatibility complex and activation antigens. Ann Neurol 1988; 24: 523–31.

Hendrickx DA, Koning N, Schuurman KG, van Strien ME, van Eden CG, Hamann J, et al. Selective upregulation of scavenger receptors in and around demyelinating areas in multiple sclerosis. J Neuropathol Exp Neurol 2013; 72: 106–18.

Hendrickx DAE, van Scheppingen J, van der Poel M, Bossers K, Schuurman KG, van Eden CG, et al. Gene expression profiling of multiple sclerosis pathology identifies early patterns of demyelination surrounding chronic active lesions. Front Immunol 2017; 8: 1810.

van Horssen J, Bö L, Vos CMP, Virtanen I, de Vries HE. Basement membrane proteins in multiple sclerosis-associated inflammatory cuffs: potential role in influx and transport of leukocytes. J Neuropathol Exp Neurol 2005; 64: 722–9.

Konjevic Sabolek M, Held K, Beltrán E, Niedl AG, Meinl E, Hohlfeld R, et al. Communication of CD8 + T cells with mononuclear phagocytes in multiple sclerosis. Ann Clin Transl Neurol 2019; 6: 1151–64.

Kumar BV, Ma W, Miron M, Granot T, Guyer RS, Carpenter DJ, et al. Human tissue-resident memory T cells are defined by core transcriptional and functional signatures in lymphoid and mucosal sites. Cell Rep 2017; 20: 2921–34.

Louveau A, Da Mesquita S, Kipnis J. Lymphatics in neurological disorders: a neuro-lympho-vascular component of multiple sclerosis and Alzheimer's disease? Neuron 2016; 91: 957–73.

Louveau A, Smirnov I, Keyes TJ, Eccles JD, Rouhani SJ, Peske JD, et al. Structural and functional features of central nervous system lymphatic vessels. Nature 2015; 523: 337–41.

Luchetti S, Fransen NL, van Eden CG, Ramaglia V, Mason M, Huitinga I. Progressive multiple sclerosis patients show substantial lesion activity that correlates with clinical disease severity and sex: a retrospective autopsy cohort analysis. Acta Neuropathol 2018; 135: 511–28.

Machado-Santos J, Saji E, Tröscher AR, Paunovic M, Liblau R, Gabriely G, et al. The compartmentalized inflammatory response in the multiple sclerosis brain is composed of tissue-resident CD8 + T lymphocytes and B cells. Brain 2018; 141: 2066–82.

Mahad DH, Trapp BD, Lassmann H. Pathological mechanisms in progressive multiple sclerosis. Lancet Neurol 2015; 14: 183–93.

Maurice C, Schneider R, Kiehl T-R, Bavi P, Roehrl MHA, Mason WP, et al. Subacute CNS demyelination after treatment with nivolumab for melanoma. Cancer Immunol Res 2015; 3: 1299–302.

McFarland H, Stone L, Calabresi P, Maloni H, Bash C, Frank J. MRI studies of multiple sclerosis: implications for the natural history of the disease and for monitoring effectiveness of experimental therapies. Mult Scler J 1996; 2: 198–205.

Merlini M, Kirabali T, Kulic L, Nitsch RM, Ferretti MT. Extravascular CD3 + T cells in brains of Alzheimer's disease patients correlate with tau but not with amyloid pathology: an immunohistochemical study. Neurodegener Dis 2018; 18: 49–56.

Mizee MR, Miedema SSM, van der Poel M, Adelia Schuurman KG, van Strien ME, et al. Isolation of primary microglia from the human post-mortem brain: effects of ante- and post-mortem variables. Acta Neuropathol Commun 2017; 5: 16.

Mueller SN, Mackay LK. Tissue-resident memory T cells: local specialists in immune defence. Nat Rev Immunol 2016; 16: 79–89.

van Nierop GP, van Luijn MM, Michels SS, Melief M-J, Janssen M, Langerak AW, et al. Phenotypic and functional characterization of T cells in white matter lesions of multiple sclerosis patients. Acta Neuropathol 2017; 134: 383–401.

van der Poel M, Ulas T, Mizee MR, Hsiao C-C, Miedema SSM, Adelia, et al. Transcriptional profiling of human microglia reveals grey–white matter heterogeneity and multiple sclerosis-associated changes. Nat Commun 2019; 10: 1139.

Prineas J. Paramyxovirus-like particles associated with acute demyelination in chronic relapsing multiple sclerosis. Science 1972; 178: 760–3.

Prineas JW, Wright RG. Macrophages, lymphocytes, and plasma cells in the perivascular compartment in chronic multiple sclerosis. Lab Invest 1978; 38: 409–21.

Revesz T, Kidd D, Thompson AJ, Barnard RO, McDonald WI. A comparison of the pathology of primary and secondary progressive multiple sclerosis. Brain 1994; 117: 759–65.

Schindelin J, Arganda-Carreras I, Frise E, Kaynig V, Longair M, Pietzsch T, et al. Fiji: an open-source platform for biological-image analysis. Nat Methods 2012; 9: 676–82.

Schøller AS, Fonnes M, Nazerai L, Christensen JP, Thomsen AR. Local antigen encounter is essential for establishing persistent CD8 + T-cell memory in the CNS. Front Immunol 2019; 10: 351.

Serafini B, Rosicarelli B, Magliozzi R, Stigliano E, Aloisi F. Detection of ectopic B-cell follicles with germinal centers in the meninges of patients with secondary progressive multiple sclerosis. Brain Pathol 2004; 14: 164–74.

Shwetank FE, Mockus TE, Ren HM, Toprak M, Lauver MD, et al. PD-1 dynamically regulates inflammation and development of brain-resident memory CD8 T cells during persistent viral encephalitis. Front Immunol 2019; 10: 783.

Smolders J, Heutinck KM, Fransen NL, Remmerswaal EBM, Hombrink P, ten Berge IJM, et al. Tissue-resident memory T cells populate the human brain. Nat Commun 2018; 9: 4593.

Smolders J, Remmerswaal EBM, Schuurman KG, Melief J, Van Eden CG, Van Lier RAW, et al. Characteristics of differentiated CD8 + and CD4 + T cells present in the human brain. Acta Neuropathol 2013; 126: 525–35.

Soares A, Govender L, Hughes J, Mavakla W, de Kock M, Barnard C, et al. Novel application of Ki67 to quantify antigen-specific in vitro lymphoproliferation. J Immunol Methods 2010; 362: 43–50.

Sørensen TL, Tani M, Jensen J, Pierce V, Lucchinetti C, Folcik VA, et al. Expression of specific chemokines and chemokine receptors in the central nervous system of multiple sclerosis patients. J Clin Invest 1999; 103: 807–15.

Sorokin L. The impact of the extracellular matrix on inflammation. Nat Rev Immunol 2010; 10: 712–23.

Steinbach K, Vincenti I, Egervari K, Kreutzfeldt M, Van Der Meer F, Page N, et al. Brain-resident memory T cells generated early in life predispose to autoimmune disease in mice. Sci Transl Med 2019; 11.

Steinert EM, Schenkel JM, Fraser KA, Beura LK, Manlove LS, Igyártó BZ, et al. Quantifying memory CD8 T cells reveals regionalization of immunosurveillance. Cell 2015; 161: 737–49.

Szabo PA, Miron M, Farber DL. Location, location, location: tissue resident memory T cells in mice and humans. Sci Immunol 2019; 4: eaas9673.

Tanaka R, Iwasaki Y, Koprowski H. Ultrastructural studies of perivascular cuffing cells in multiple sclerosis brain. The American Journal of Pathology 1975; 81: 467–78.

Thompson AJ, Baranzini SE, Geurts J, Hemmer B, Ciccarelli O. Multiple sclerosis. Lancet 2018; 391: 1622–36.

Topham DJ, Reilly EC. Tissue-resident memory CD8 + T cells: from phenotype to function. Front Immunol 2018; 9: 515.

van Unen V, Höllt T, Pezzotti N, Li N, Reinders MJT, Eisemann E, et al. Visual analysis of mass cytometry data by hierarchical stochastic neighbour embedding reveals rare cell types. Nat Commun 2017; 8: 1740.

Vollmer T. The natural history of relapses in multiple sclerosis. J Neurol Sci 2007; 256: S5–S13.

Wagner CA, Roqué Pj, Mileur TR, Liggitt D, Goverman JM. Myelin-specific CD8 T cells exacerbate brain inflammation in CNS autoimmunity. J Clin Invest 2020; 130: 203–13.

Wakim LM, Woodward-Davis A, Bevan MJ. Memory T cells persisting within the brain after local infection show functional adaptations to their tissue of residence. Proc Natl Acad Sci USA 2010; 107: 17872–9.

Wakim LM, Woodward-Davis A, Liu R, Hu Y, Villadangos J, Smyth G, et al. The molecular signature of tissue resident memory CD8 T cells isolated from the brain. J Immunol 2012; 189: 3462–71.

Wingerchuk DM, Weinshenker BG. Disease modifying therapies for relapsing multiple sclerosis. BMJ 2016; 354: i3518.

Zhu Q-B, Unmehopa U, Bossers K, Hu Y-T, Verwer R, Balesar R, et al. MicroRNA-132 and early growth response-1 in nucleus basalis of Meynert during the course of Alzheimer's disease. Brain 2016; 139: 908–21.

Zotova E, Bharambe V, Cheaveau M, Morgan W, Holmes C, Harris S, et al. Inflammatory components in human Alzheimer's disease and after active amyloid-β42 immunization. Brain 2013; 136: 2677–96.